

# Journal of Materials Chemistry A

Accepted Manuscript



This is an *Accepted Manuscript*, which has been through the Royal Society of Chemistry peer review process and has been accepted for publication.

*Accepted Manuscripts* are published online shortly after acceptance, before technical editing, formatting and proof reading. Using this free service, authors can make their results available to the community, in citable form, before we publish the edited article. We will replace this *Accepted Manuscript* with the edited and formatted *Advance Article* as soon as it is available.

You can find more information about *Accepted Manuscripts* in the [Information for Authors](#).

Please note that technical editing may introduce minor changes to the text and/or graphics, which may alter content. The journal's standard [Terms & Conditions](#) and the [Ethical guidelines](#) still apply. In no event shall the Royal Society of Chemistry be held responsible for any errors or omissions in this *Accepted Manuscript* or any consequences arising from the use of any information it contains.



21 **Abstract:** Adsorption represents an efficient and economical approach for water purification and  
22 substantial research are being performed to developing effective sorbent materials. Porous boron  
23 nitride (BN) composed of light elements is considered as a promising candidate for pollution  
24 treatment due to its unique polarity of B-N bonds, high specific surface area, numerous structural  
25 defects, chemical stability, and oxidation resistance. However, adsorption performance based on  
26 porous BN is hindered by either few activated sites or low degree of crystallinity. In this work,  
27 we have developed a simple chemical method to activate pre-obtained well-crystallized porous  
28 BN fibers in acid solution. The successful chemical activation has been identified by FTIR  
29 spectra and zeta potential measurement. Benefiting from these advantageous features, the  
30 activated BN fibers with high stability exhibited enhanced cationic dye removal performance  
31 compared to the un-activated ones. The effects of pH value, contact time, temperature and  
32 adsorbent amount on the methylene blue (MB) adsorption properties were analyzed. The  
33 adsorption equilibrium data were interpreted in terms of the Langmuir and Freundlich models  
34 and the results showed that Langmuir isotherms best represent the adsorption system. The  
35 maximum adsorbed amount for MB was high up to 392.2 mg/g at pH 8.0 and 30 °C. The  
36 adsorption rate was sharply enhanced after chemical activation. The excellent reusability of the  
37 activated BN was also confirmed. It is shown that the chemical activation plays a key role in  
38 enhanced dye adsorption performance. Therefore, our developed chemical activation method for  
39 porous BN fibers opens the door toward to the practical activated BN for drinking water  
40 purification.

41

## 42 1. Introduction

43  
44 Environmental pollution problem has attracted great attention because many industries such as  
45 dye manufacturing and printing have produced highly coloured effluents, and disposal of these  
46 wastes into water has resulted in larger volume of dye wastewaters <sup>1</sup>. The coloured effluents not  
47 only lead to organic load and toxicity to the environment, but also impede light penetration to  
48 affect aquatic ecosystems <sup>2</sup>. The adsorption has been found to be superior as compared to other  
49 traditional treatment methods for wastewater treatment due to its low-cost, easy availability,  
50 simplicity of design, high efficiency, ease of operation and ability to treat hazardous dyes and  
51 metal ions <sup>3, 4</sup>. Various adsorbents have been applied for the hazardous dyes removal from  
52 aqueous solution, including activated carbon <sup>5</sup>, fly ash and red mud <sup>6</sup>, mesoporous  
53 aluminophosphate <sup>7</sup>, free-standing carbonaceous nanofiber membranes <sup>8</sup>, magnetic powder  
54 MnO-Fe<sub>2</sub>O<sub>3</sub> composite <sup>9</sup>, and porous CeO<sub>2</sub> <sup>10</sup>. However, the high-quality adsorbents with high  
55 removal capacity and reusability are still required. Compared with the traditional carbon material,  
56 BN can be considered as promising adsorbent due to their highly stability in harsh conditions,  
57 which enables more treatment technique for recycled usage<sup>11, 12</sup>.

58 Very recently, several kinds of porous BN nanostructured materials have been successfully  
59 fabricated, and their applications in water purification and treatment have been extensively  
60 investigated due to their high specific surface area, numerous density defects and large void  
61 volume<sup>13-15</sup>. Specially, activated BN has also been developed by our group to improve their  
62 adsorption performance, in which more crystal defects and hydroxyl or organic surface groups  
63 have been introduced via the presence of P123 (poly(ethylene glycol)-poly(propylene glycol)-  
64 poly(ethylene glycol)) as a activating reagent <sup>16</sup>. Note that the obtained activated BN is not only  
65 short of stability in very harsh conditions due to their poor degree of crystallinity, but also

66 contains many impurities because of the introduction of P123. Hence these shortcomings such as  
67 instability and lack of numerous adsorption sites need to overcome to further improve their  
68 performance in wastewater treatment. Herein, we report a kind of novel porous BN fibers with  
69 high crystallinity and abundant activated sites via a two-step synthesis route, which exhibited  
70 greatly improved cationic dye removal performance. Firstly, BN fibers with high degree of  
71 crystallinity were prepared by using boric acid and melamine as the starting reactants in  $\text{NH}_3$   
72 flow at a high temperature. Secondly, a new chemical activation pretreatment was utilized to  
73 activate as-received BN fibers to obtain numerous surface functional groups and defects, so as to  
74 increase their adsorption capacity. The resultant adsorbents were subsequently tested in the  
75 removal of cationic dyes in different experimental conditions to confirm the validation of  
76 chemical activation to enhance adsorption capacity (up to 392.2 mg/L) and uptake rate.  
77 Langmuir and Freundlich isotherms models have been used to further analyze the adsorption  
78 data. Furthermore, the removal efficiency of  $\sim 94\%$  was still retained even after fifteen  
79 adsorption-regeneration cycles. A thorough knowledge of activated BN enables the preparation  
80 of adsorbents with appropriate characteristic for drinking water purification.

## 81 **2. Experimental**

### 82 **2.1. Material Synthesis**

83 Analytical grade  $\text{H}_3\text{BO}_3$  and  $\text{C}_3\text{N}_6\text{H}_6$  were used directly without further purification as  
84 starting materials to synthesize porous BN fibers. Methylene blue, as a model cationic dye  
85 contained the aromatic rings, was used to study the hazardous dye removal nature of activated  
86 BN. Table S1 and Figure S1 (Supporting Information) exhibit the property and structure of  
87 cationic dye MB. A mixture of  $\text{H}_3\text{BO}_3$  and  $\text{C}_3\text{N}_6\text{H}_6$  at a molar ratio of 1:2 was dissolved in 300

88 ml of the distilled water. The reaction mixtures were heated and kept at a boiling state to  
89 completely evaporate of the distilled water. The white precipitate ( $C_3N_6H_6 \cdot 2H_3BO_3$ , M·2B) was  
90 obtained. Subsequently, the precursors were treated through a multi-stage heat process to  
91 produce BN fibers in an alumina tube using a resistance-heating horizontal furnace. Firstly, the  
92 precursors were calcined at 546°C for 2 h (ramp rate 5°C/min). Secondly, they were heated at  
93 1560 °C for 4 h at a heating rate of 10 °C/min. All reaction was carried out in a flow of  $NH_3$  (200  
94 ml/min).

95 The activation process was carried out by adding 3g of above obtained BN fibers into 50%  
96 (w/w) of the activating reagent (1 M  $H_2SO_4$  aqueous solution and 8 M  $HNO_3$  aqueous solution  
97 mixed together with their weight ratio of 1:1). After sonication for 30 min at room temperature,  
98 the obtained slurry was mechanically stirred in an 80 °C water bath for 2 h. After activation, the  
99 sample was washed with deionized water for several times until the pH of the rinse became  
100 neutral (pH 6.8-7.2), following by drying at 105 °C for 24 h. The sample prepared was labeled as  
101 activated BN.

## 102 **2.2. Characterization techniques**

103 The structure of the samples was examined using X-ray powder diffraction (XRD, BRUKER  
104 D8 FOCUS) analysis. Fourier transformer infrared (FTIR) spectra were recorded on a Nicolet  
105 7100 spectrophotometer between 400 and 4000  $cm^{-1}$ . Transmission electron microscopy (TEM)  
106 experiments were performed on a Tecnai F20 electron microscope (Philips, Netherlands) with an  
107 acceleration voltage of 200 kV. The nitrogen physisorption isotherms were measured at -196 °C  
108 on an AutoSorb iQ-C TCD analyzer. Prior to the measurement, the samples were activated in  
109 vacuum at 300 °C for 3 h. The Brunauer-Emmett-Teller (BET) specific surface area was

110 calculated from the nitrogen adsorption data in the relative pressure ranging from 0.01 to 0.3.  
111 The pH values of the solutions were measured by pH meter (PHS-25, Hangzhou). A double  
112 beam UV/vis spectrophotometer (HITACHI, U-3900H) was used to determine the concentration  
113 of dye samples. The thermostability of the products was tested by simultaneous thermal analysis  
114 (SDT-Q600). Conventional elemental analyzers (Leco, TC500 and CS230, USA) were applied to  
115 analyze the detailed N, O, and C contents of the two adsorbents, respectively. X-ray  
116 photoelectron spectroscopy (XPS) measurement was performed in an ultrahigh vacuum with a  
117 VG ESCALAB 210 electron spectrometer equipped with a multichannel detector.

### 118 ***2.3. Adsorption experiment***

119 For all adsorption experiments in this work, the studies were carried out in glass flask with a  
120 magnetic stirrer. Stock solution (100 mg/L) of MB dye was prepared via adding MB dyes (100  
121 mg) into 1 L of distilled water, which acts as the source for dissolution. The mixtures were  
122 continuously stirred by a magnetic stirrer at 150 rpm, and then centrifuged and filtered. For the  
123 adsorption rate tests, 250 ml of MB solution at the initial concentration of 25 mg/L and 60 mg  
124 adsorbents were used. The solution pH was adjusted to 8. The two adsorbents were taken at  
125 different time intervals. In order to obtain the maximum removal of MB over the two adsorbents,  
126 optimized conditions, such as contact time, adsorbent dosage and contact temperature, and pH  
127 value, were investigated. In the experiments of equilibrium adsorption isotherm, the solution  
128 equilibrium pH was maintained at 8, and 250 ml MB solution was mixed with the dosages of  
129 adsorbents ranging from 10 to 100 mg. The temperature effect of adsorption of MB on the  
130 activated BN and the BN fibers was measured in the range of 10-50 °C. The pH values of dye  
131 solutions were adjusted from 2 to 12 by adding amount of 0.1 M HCl or NaOH solutions,  
132 respectively. The solution concentrations (the supernatants) were determined by UV/vis

133 spectrophotometer at the corresponding  $\lambda_{max} = 663$  nm. The dye removal percentage of MB over  
134 the two adsorbents was calculated by the Equation 1

$$135 \quad \eta (\%) = (C_0 - C_e) \cdot 100 / C_0 \quad (1)$$

136 Where  $C_0$  and  $C_e$  (mg/L) are the initial solution concentration and equilibrium concentration,  $\eta$  is  
137 the dye removal percentage of MB, respectively.

#### 138 **2.4. Regeneration**

139 The regeneration of activated BN was carried out by thermal degradation method. After the  
140 filtration, the collected adsorbent containing MB was dried at 100 °C, then placed into a muffle  
141 furnace and heated at 400 °C for 1 h. the obtained adsorbent was chemically re-activated with the  
142 mixed solution of dense sulfuric acid and nitric acid for use in the further test.

### 143 **3. Results and discussion**

#### 144 **3.1. Characterization of activated boron nitride**

145 XRD patterns of the as-growth adsorbents, the activated BN and the BN fibers, are displayed in  
146 Figure 1a, respectively. Both of them display similar sharp diffraction peaks at  $2\theta = \sim 26.7^\circ$  and  
147  $\sim 43.8^\circ$ , corresponding to the (002) and (100) plane spacing of hexagonal BN<sup>17, 18</sup>. When  
148 comparing with our previously reported activated BN by P123<sup>16</sup>, as illustrated by the XRD  
149 pattern in Figure S2 (Supporting Information), currently obtained BN fibers exhibits higher  
150 degree of crystallinity. The higher crystallinity of as-obtained activated BN endows its better  
151 stability during adsorption process as sorbent, which has been further identified by the  
152 thermogravimetry measurement as shown in Figure S3 in Supporting Information. Figure 1b  
153 shows FTIR spectra of the activated BN and the BN fibers, respectively. Two main peaks at ~

154 1400 and  $\sim 800\text{ cm}^{-1}$  are verified to the B-N stretching vibrations and B-N-B bending vibrations  
155 <sup>19-22</sup>, which can be both detected in the two samples. Moreover, intensity increased vibration  
156 band of  $\sim 3420\text{ cm}^{-1}$  (B-NH<sub>2</sub>) and a new emerging peak located at  $\sim 3250\text{ cm}^{-1}$  (B-OH) can be  
157 observed in the activated BN <sup>14, 20</sup>. We deduce it should be ascribed to the chemical activation  
158 process, which facilitates functionalization of hydroxyl and organic groups (B-NH<sub>2</sub>/B-OH) on  
159 the BN fibers. Besides, additional surface bonds were also measured on the surface of activated  
160 BN, i.e. B-N-O and B-N-O <sup>20</sup>. In addition, XPS spectra and elemental analysis further suggest  
161 that the possible functional groups were introduced onto the surface of the as-prepared BN fibers  
162 via chemical activation, as shown in Figure S4 and Table S3 (Supporting Information). The  
163 external morphology and microstructures of the activated BN and the BN fibers were  
164 investigated by TEM, as displayed in Figure 1(c,d). As compared in the rectangle regions in  
165 Figure 1c and 1d, BN fibers exhibit smooth edges in the TEM image, whereas the edges of  
166 activated BN are rather rough, suggesting numerous surface defects were introduced after  
167 chemical activation. Taking into account of the unchanged crystal structures of two kinds of  
168 porous BN fibers as shown in Figure 1a, the chemical activation reaction should mainly take  
169 place on surface rather than inside.

170 The possible activated reaction schemes of the BN fibers by the treatment of the mixed acid  
171 solution are provided in Figure 2. Because the melamine was selected as one of the starting  
172 reactants, the decomposition of melamine resulted in the presence of carbonaceous composition in  
173 the as-prepared BN fibers <sup>23</sup>. It is known that carbonaceous composition could be removed from  
174 the lattice and/or surface of BN via the reaction with dense nitric acid at 80 °C (reaction equation  
175 (1) of Figure 2). This reaction is helpful to improve the number of defects, the specific surface area,  
176 and the pore volume, as illustrated in Figure 1d and 2. The addition of sulfuric acid can

177 accelerate the rate of the reaction 1 by capturing water. A high-concentration acidic solution  
178 creates sufficient oxidized radicals on the BN fibers surface, as displayed in reaction equation (2)  
179 of Figure 2<sup>24</sup>. The reaction equation (3) of Figure 2 shows that a low-concentration solution  
180 results in the formation of functional groups on the BN fibers surface<sup>25</sup>. Therefore, chemical  
181 activation to the BN fibers via the mixed solution of sulfuric acid and nitric acid is favorable to  
182 introducing functional groups and defects onto the surface, which can enhance the adsorption  
183 ability of the activated BN.

184 Figure 3 illustrates nitrogen adsorption/desorption isotherms (-196 °C) and the corresponding  
185 pore size distributions of the two adsorbents, respectively. The measured isotherms (Figure 3a)  
186 can be classified as type I isotherm according to the IUPAC nomenclature, and exhibit a H4 type  
187 broad hysteresis loop. Since type I isotherm and Type H4 loops also indicate that the pores  
188 contain microporosity and narrow slit-shaped mesopores, we use a Non-Local Density  
189 Functional Theory (NLDFT) method to determine the pore widths and size distribution for the  
190 activated BN and the BN fibers, respectively<sup>23, 26</sup>. Both samples exhibit a broad pore size  
191 distribution (PSD), as shown in Figure 3b, which are given a bimodal distribution with the main  
192 characteristic pore sizes of ~1.3 and ~3.9 nm. Comparing with both curves, we clearly observe  
193 that the surface area of the activated BN slightly increased from 1045 to 1104 m<sup>2</sup>/g when  
194 activated by activating reagent. Accordingly, the pore volumes also increased from 0.57 to 0.63  
195 cm<sup>3</sup>/g. Therefore, the activation process influences its specific surface area and pore volume  
196 simultaneously without destruction of their integrity.

197 To further identify the validity of activation, their surface charge conditions were monitored  
198 by zeta potential. Figure 4 show that the activated BN had an overall negative surface charge at  
199 above pH 2, whereas the BN fibers exhibited almost an overall neutral charge even at pH 8. In

200 addition, the zeta-potential of activated BN rise as pH value increase due to protonation of the  
201 hydroxyl and amino groups on the surface. Therefore, one can say that the chemical activation  
202 leads to more negative charge surface, which come from the induced functional groups and  
203 defects. Accordingly, more negative charge results in enhancement of the electrostatic attraction  
204 between the activated BN and the pollution dye molecules.

### 205 *3.2. Adsorption studies*

206 Considering its porous structure with high specific surface area also with more negative  
207 charges, the as-obtained chemical activated BN fibers should have an excellent adsorption  
208 activity when used as a sorbent in wastewater treatment. To demonstration the potential  
209 applicability of the present activated BN fibers in these applications, we investigated its  
210 adsorption activity for the removal of MB in aqueous solutions relative to that of the untreated  
211 one. MB adsorption capacity was observed to be excellently up to 392.2 mg/g. Furthermore, the  
212 extremely rapid adsorption was observed that the residual dye was just 1.5 wt % within 5 min  
213 and 0.2 wt % within 30 min, respectively, when 20 mg of activated BN was applied in a 250 ml  
214 of the dye solution (25 mg/L) at 30 °C and pH value of 8. The effect of removal of MB depends  
215 on the experimental parameters, such as the characteristic of the adsorbents, contact time, pH  
216 value, adsorption temperature, etc. Therefore, these experimental parameters are optimized with  
217 the aim of achieving maximum adsorption.

218 Figure 5a exhibits the rates of MB adsorption on the activated BN and the BN fibers obtained  
219 by batch contact time studies with an initial MB concentration of 25 mg/L and the adsorbents of  
220 60 mg at pH of 8, respectively. It is worthy to note that, for the activated BN, the removal was  
221 very fast during the first 5 min, and then the equilibrium was reached within 30 min. In addition,

222 the adsorption capacities onto the two adsorbents were in the order of the activated BN > the BN  
223 fibers. The fast adsorption reveals a high complexation rate between the activated BN and the  
224 dye molecules, which is correlated to its surface defects and hydroxyl and organic groups on the  
225 surface. More hydroxyl and organic groups and surface defects are favorable for the diffusion of  
226 dye molecules onto much more activated sites within a shorter time<sup>27</sup>.

227 The MB adsorption as a function of the activated BN dosage (10-100 mg) at pH of 8 is  
228 depicted in Figure 5b. The adsorption percentage of MB rise with the increase of activated BN  
229 dosage since the increase of adsorbent dosage enlarged the surface area and activated sites for  
230 adsorption. The adsorption of MB on the BN fibers is also displayed in Figure 5b as a  
231 comparison. It clearly indicates that the removal percentage on the BN fibers was much lower  
232 than that of MB on the activated BN under same experimental conditions. The chemical  
233 activation process leads to improving number of hydroxyl and amino groups and surface defects,  
234 which work as mainly effective sites for adsorption leading higher adsorption capacity.

235 The effect of temperature on adsorption of MB is analyzed at temperatures ranging from 10-  
236 50 °C, which is shown in Figure 5c. The removal percentage of MB using activated BN  
237 increased with increasing temperature from 10 to 30°C, suggesting that the adsorption process is  
238 endothermic. The temperature has two major effects on the adsorption process. On one hand,  
239 increasing the temperature contributes to the decrease of the solution viscosity, and in turn,  
240 results in the increase of diffusion rate for the adsorbate molecules across the external boundary  
241 layer and the internal pores of the activated BN. On the other hand, changing the temperature  
242 also elevates the equilibrium capacity between the absorbent and adsorbate in the solution.  
243 However, with the further increase of the temperature up to 50°C, the adsorption percentage of  
244 MB quickly decreased. This is mainly because increasing the temperature weakens the

245 interactions between the activated BN and MB, and hinders the MB adsorption. The temperature  
246 effect on the adsorption of un-activated BN fibers also exhibits the similar phenomenon as  
247 shown.

248 We also detected the effect of pH value of the MB solution on the adsorption amount of the  
249 two sorbents. Figure 5d indicates that the removal ability of MB has been enhanced with the  
250 increase of pH value and reaches the maximum point at pH value of 8, which is consistent with  
251 the zeta-potential results (Figure 4). In the process of adsorption, the heterocharge between the  
252 adsorbate and adsorbent is favorable for adsorbing reaction. More protons are available on the  
253 surface of the adsorbents when  $\text{pH} < 7$ , which lead to decreasing negative charges of adsorbent  
254 surface<sup>28</sup>. Additionally, the protonate amino groups of MB create repulsive force with the  
255 electron deficient boron active sites of the activated BN, so the adsorption capacity increases  
256 with rise of pH value<sup>7</sup>. A weakly alkaline environment is in favor of the adsorption of MB since  
257 the surface of activated BN may occupy more negatively charged  $\text{OH}^-$  ions. However, the  
258 adsorption amount decreases gradually when  $\text{pH} > 8$ , owing to the excessive negatively charged  
259  $\text{OH}^-$  ions in the solution blocking the beneficial effects of that of the surface<sup>9,27</sup>.

260 To verify the great advantages of negatively-charged activated BN adsorbing cationic dye  
261 molecules by electrostatic interaction, we compare the adsorption performance based on neutral  
262 (neutral red) and anionic (methyl orange) dyes. Figure 6 (a,b) shows that the adsorption rate and  
263 capacity of methylene blue onto the activated BN is much higher than that of neutral red and  
264 methyl orange, respectively. Additionally, after deactivation by ammonia treatment at 900 °C,  
265 the adsorption rate and capacity of methylene blue of the resultant BN (deactivated BN) is much  
266 lower than that of the activated BN, as illustrated in Figure 6c and 6d. We notice that the  
267 deactivated BN still exhibits a high surface area of 1100  $\text{m}^2/\text{g}$  and a large pore volume of 0.62

268 cm<sup>3</sup>/g. This deactivation reaction only resulted in less negative charge surface (the zeta-potential  
269 of the deactivated BN was almost zero even at pH 7). Therefore, the strong electrostatic  
270 interaction between methylene blue and activated BN is believed to be the key point causing the  
271 high adsorption rate and capacity.

272 The adsorption isotherm is one of the most useful methods to understand the mechanisms of  
273 the adsorption process, to detect how the adsorbent interacts with the adsorbate and to evaluate  
274 the application of the process. Figure 7 shows the adsorption isotherms of MB onto the surface  
275 of two sorbents at pH 8 and 30 °C. In the entire concentration range from 0.38 to 20 mg/L, the  
276 adsorption capacities of MB on the two adsorbents are in the order of activated BN > BN fibers.  
277 This order is the same as that of the influences of contact time, adsorbent dosage, contact  
278 temperature, and pH value mentioned above. The maximum adsorption capacities are 392.2  
279 mg/g for activated BN and 243.2 mg/g for BN fibers, respectively. The different adsorption  
280 capacities for activated and un-treated ones might be the overall effects of electrostatic  
281 interactions, which have significant difference in surface charges. It worth noting that the  
282 maximum value of adsorption capacity for the present activated BN (392.2 mg/g) is remarkably  
283 larger than those of most common commercial and state-of-the-art sorbents <sup>7, 11, 14, 15, 29-31</sup>.  
284 Specially, the adsorption capacity and rate of the activated BN for methylene blue are about 2  
285 and 10 times higher than that of the commercial activated carbon, respectively <sup>8</sup>. The improved  
286 adsorption ability of the activated BN mainly ascribes to the chemical activation via the mixed  
287 solution, which is favorable to introducing functional groups and defects onto the surface. The  
288 result suggests the excellent adsorption capacity in our newly prepared activated BN material.

289 Since the surface of the BN fibers is negatively charged, the chosen cationic dye MB can be  
290 adsorbed by the electrostatic interactions. The observed high adsorption capacity of activated BN

291 mainly originates from the following several aspects. For BN, the polar B-N bond is suitable for  
292 the MB chemisorption, because the BN fibers exhibit the “lop-sided” densities characteristic of a  
293 considerable degree of ionic B-N bonding, and the polyelectron nitride can transfer more  
294 electron density to cationic dye<sup>32</sup>. After activation, the activated BN has an overall negative  
295 surface charge at above pH 2, which can easily adsorb positively charged dye. The porous BN  
296 has high specific surface area of 1104 m<sup>2</sup>/g and large pore volume (0.63 cm<sup>3</sup>/g) also facilitates  
297 the adsorption<sup>33,34</sup>. Most importantly, much more activated sites in the activated BN can lead to  
298 a great enhancement of the MB adsorption due to the high density structural defects and  
299 numerous hydroxyl and amino groups, which could offer strong binding sites and enhancing the  
300 dissociation of MB on BN fibers.

301 The Langmuir adsorption isotherm has been widely used to investigate the adsorption process  
302 of pollutants from the liquid solutions<sup>33</sup>. It assumes that the adsorption of pollutants takes place  
303 in the specific homogeneous sites within the adsorbents, and many successful monolayer  
304 adsorptions have been found. The Langmuir isotherm is represented in the form as (Equation 2)

$$305 \quad Q_e = Q_m K C_e / (1 + K C_e). \quad (2)$$

306 Where  $Q_e$  is the adsorbed amount of dyes on the equilibrium concentration (mg/g),  $C_e$  is the  
307 equilibrium concentration in solution (mg/L),  $Q_m$  is the maximum adsorption capacity  
308 corresponding to complete monolayer covering on the adsorbents (mg/g), and  $K$  is the  
309 equilibrium constant related to the free energy of adsorption.

310 The Freundlich isotherm is an empirical equation, which has usually been employed to  
311 represent the heterogeneous systems<sup>9</sup>. The Freundlich equation is written as (Eq. 3)

$$312 \quad Q_e = K C_e^{1/n}. \quad (3)$$

313 Where,  $K$  and  $n$  are the Freundlich adsorption constants, which indicate that the extent of the  
314 adsorption and the degree of nonlinearity between adsorption and solution concentration,  
315 respectively.

316 Figure 7 reveals that the Langmuir model had well fit with the experimental data for the two  
317 adsorbents in the order of activated BN > BN fibers with the correlation coefficients ( $R^2$ ) of  
318 0.998 and 0.993, respectively (Table S2, Supporting Information). While for the Freundlich  
319 model, the correlation coefficients ( $R^2$ ) of activated BN and the BN fibers were 0.916 and 0.92,  
320 respectively. This result also reveals that all sites were equal (equal energies and enthalpies).  
321 Moreover, we note that the curve for activated BN had a very high slope in the initial portion and  
322 then level off, revealing that the activated BN possesses incredible adsorption density even at  
323 low equilibrium hazardous dye concentrations and high affinity for MB molecules. Hence, this is  
324 suitable for lowering hazardous dye concentration by adsorption in wastewater.

### 325 ***3.3. Regeneration of activated boron nitride***

326 As known, the feasibility of applying the adsorbent systems in large-scale operations is  
327 determined by the cost of their disposal or regeneration. The high-temperature calcination  
328 method has been paid extensive attention because it is a feasible disposal and energy-saving  
329 process. Due to its high thermal stability, a simple regeneration experiment (calcining at 400 °C  
330 for 1 h in air) was carried out for the removal of adsorbed MB and the regeneration of activated  
331 BN. Batches of regeneration experiment for 10 activated BN samples were carried out to  
332 evaluate their cycle property for MB removal. The removal efficiency of about 94 % was still  
333 retained even after 15 runs, as presented in Figure 8, which is higher than that of the activated  
334 BN reported in our previous work<sup>16</sup>. And then the removal efficiency has no obvious change

335 with further increasing of cycles. It should be noticed that the decrease of adsorption efficiency  
336 after several cycles dose not ascribe to the deactivation, due to the low temperature regeneration  
337 process. In addition, the activated BN still exhibits excellent removal capacity of methylene blue  
338 even when  $\text{pH} < 3$  or  $\text{pH} > 11$  due to its novel properties, which enables its actual applications in  
339 harsh conditions.

340

#### 341 **4. Conclusions**

342 In summary, the activated BN with high adsorption capacity and degree of crystallinity were  
343 synthesized by a two-step synthesis route. Chemical activation of the BN fibers via using the  
344 mixed solution of sulfuric acid and nitric acid as activating reagent assisted by ultrasonication  
345 increases their hydroxyl and organic groups and surface defects. The activated BN exhibited  
346 excellent adsorption capacity as high as 392.2 mg/L and adsorption rate (effectively eliminating  
347 ~98.5 wt % within 5 min) at 30 °C and pH value of 8 for the cationic dyes. Compared with the  
348 BN fibers, the removal of MB on the activated BN was greatly improved. Moreover, only 6%  
349 efficiency lost after fifteen cycles. Therefore, we believe that the activated BN is a very  
350 promising candidate for hazardous dyes removal from aqueous solution, and open a door for  
351 increasing dyes adsorption weight density in the BN system, by more considerations on chemical  
352 activation.

353

#### 354 **Acknowledgements**

355 This work was supported by the National Natural Science Foundation of China (51332005,  
356 51372066, 51172060, 51202055, 21103056, 51402086), the Program for Changjiang Scholars

357 and Innovative Research Team in University (PCSIRT: IRT13060), the Australian Research  
358 Council, the Hundred Talents Program of Hebei Province (E2014100011), the Natural Science  
359 Foundation of Hebei Province (Grant No. E2012202040), the Tianjin Research Program of  
360 Application Foundation and Advanced Technology (14JCYBJC42200), and the Innovation Fund  
361 for Excellent Youth of Hebei University of Technology (No.2012001).

362

363

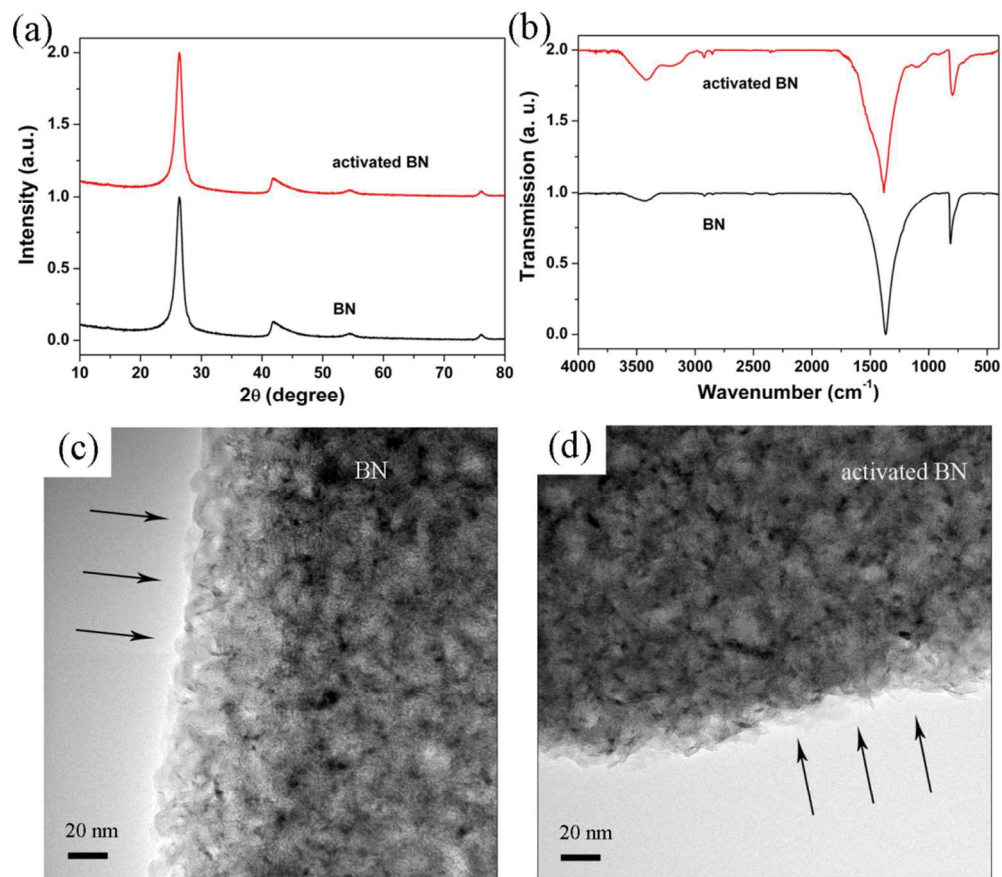
## 364 Notes and references

- 365 1. S. J. Allen, G. McKay and J. F. Porter, *J. Colloid Interf. Sci.*, 2004, **280**, 322-333.  
366 2. C. K. Lee, K. S. Low and P. Y. Gan, *Environ. Technol.*, 1999, **20**, 99-104.  
367 3. S. Babel and T. A. Kurniawan, *J. Hazard. Mater.*, 2003, **97**, 219-243.  
368 4. J. Li, R. Lu, B. Dou, C. Ma, Q. Hu, Y. Liang, F. Wu, S. Qiao and Z. Hao, *Environ. Sci.*  
369 *Technol.*, 2012, **46**, 12648-12654.  
370 5. A. J. Brooks, L. Hyung-nam and E. K. James, *Nanotechnology*, 2012, **23**, 294008.  
371 6. S. Wang, Y. Boyjoo, A. Choueib and Z. H. Zhu, *Water Res.*, 2005, **39**, 129-138.  
372 7. C. Kannan, K. Muthuraja and M. R. Devi, *J. Hazard. Mater.*, 2013, **244-245**, 10-20.  
373 8. H. W. Liang, X. Cao, W. J. Zhang, H. T. Lin, F. Zhou, L. F. Chen and S. H. Yu, *Adv.*  
374 *Funct. Mater.*, 2011, **21**, 3851-3858.  
375 9. R. Wu, J. Qu and Y. Chen, *Water Res.*, 2005, **39**, 630-638.  
376 10. X. H. Lu, D. Z. Zheng, J. Y. Gan, Z. Q. Liu, C. L. Liang, P. Liu and Y. X. Tong, *J.*  
377 *Mater. Chem.*, 2010, **20**, 7118-7122.  
378 11. G. Lian, X. Zhang, S. Zhang, D. Liu, D. Cui and Q. Wang, *Energy Environ. Sci.*, 2012, **5**,  
379 7072-7080.  
380 12. X. Zhang, G. Lian, S. Zhang, D. Cui and Q. Wang, *CrystEngComm*, 2012, **14**, 4670-  
381 4676.  
382 13. L. L. Xue, B. Z. Lu, Z. S. Wu, C. H. Ge, P. Wang, R. Zhang and X. D. Zhang, *Chem.*  
383 *Eng. J.*, 2014, **243**, 494-499.  
384 14. J. Li, J. Lin, X. Xu, X. Zhang, Y. Xue, J. Mi, Z. Mo, Y. Fan, L. Hu, X. Yang, J. Zhang, F.  
385 Meng, S. Yuan and C. Tang, *Nanotechnology*, 2013, **24**, 155603.  
386 15. W. Lei, D. Portehault, D. Liu, S. Qin and Y. Chen, *Nat. Commun.*, 2013, **4**, 1777.  
387 16. J. Li, X. Xiao, X. Xu, J. Lin, Y. Huang, Y. Xue, P. Jin, J. Zou and C. Tang, *Sci. Rep.*,  
388 2013, **3**, 3208.  
389 17. F. Cao, Y. Ding, L. Chen and C. Zhang, *Nanoscale*, 2013, **5**, 10000-10006.  
390 18. W. Meng, Y. Huang, Y. Fu, Z. Wang and C. Zhi, *J. Mater. Chem. C*, 2014, **2**, 10049-  
391 10061.  
392 19. L. Wang, S. Q. Ni, C. Guo and Y. Qian, *J. Mater. Chem. A*, 2013, **1**, 6379-6387.  
393 20. C. Tang, Y. Bando, Y. Huang, C. Zhi and D. Golberg, *Adv. Funct. Mater.*, 2008, **18**,  
394 3653-3661.  
395 21. C. Zhi, Y. Bando, C. Tang, D. Golberg, R. Xie and T. Sekigushi, *Appl. Phys. Lett.*, 2005,  
396 **86**, 213110.  
397 22. C. Zhi, Y. Bando, C. Tang, H. Kuwahara and D. Golberg, *Adv. Mater.*, 2009, **21**, 2889-  
398 2893.  
399 23. Q. Weng, X. Wang, C. Zhi, Y. Bando and D. Golberg, *ACS Nano*, 2013, **7**, 1558-1565.  
400 24. Y. Ide, F. Liu, J. Zhang, N. Kawamoto, K. Komaguchi, Y. Bando and D. Golberg, *J.*  
401 *Mater. Chem. A*, 2014, **2**, 4150-4156.  
402 25. K. Possemiers, P. Van Der Voort and E. F. Vansant, *J. Chem. Soc., Faraday Trans.*,  
403 1996, **92**, 679-684.  
404 26. R. Evans and P. Tarazona, *Phys. Rev. Lett.*, 1984, **52**, 557-560.  
405 27. B. Gu, J. Schmitt, Z. Chen, L. Liang and J. F. McCarthy, *Environ. Sci. Technol.*, 1994,  
406 **28**, 38-46.  
407 28. B. Pan and B. Xing, *Environ. Sci. Technol.*, 2008, **42**, 9005-9013.  
408 29. S. Wang and Z. H. Zhu, *J. Hazard. Mater.*, 2006, **136**, 946-952.

- 409 30. X. Zhang, A. Li, Z. Jiang and Q. Zhang, *J. Hazard. Mater.*, 2006, **137**, 1115-1122.  
410 31. Q. S. Liu, T. Zheng, N. Li, P. Wang and G. Abulikemu, *Appl. Surf. Sci.*, 2010, **256**, 3309-  
411 3315.  
412 32. Z. Zhou, J. Zhao, Z. Chen, X. Gao, T. Yan, B. Wen and P. v. R. Schleyer, *J. Phys. Chem.*  
413 *B*, 2006, **110**, 13363-13369.  
414 33. M.-X. Zhu, L. Lee, H.-H. Wang and Z. Wang, *J. Hazard. Mater.*, 2007, **149**, 735-741.  
415 34. V. Vimonses, B. Jin, C. W. K. Chow and C. Saint, *J. Hazard. Mater.*, 2009, **171**, 941-  
416 947.  
417

418 **Figures and Captions:**

419



420

421 **Figure 1.** (a) XRD patterns and (b) FTIR spectra of the activated BN and the BN fibers, TEM

422 images of (c) the BN fiber and (d) the activated BN.

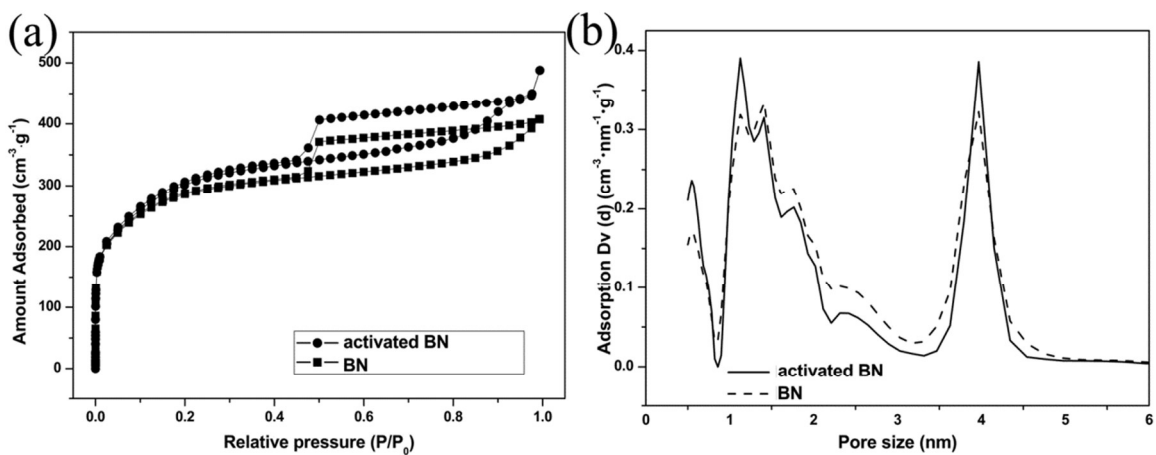
423



424

425 **Figure 2.** Chemically activated reactions of the BN fibers in the mixed acid solution.

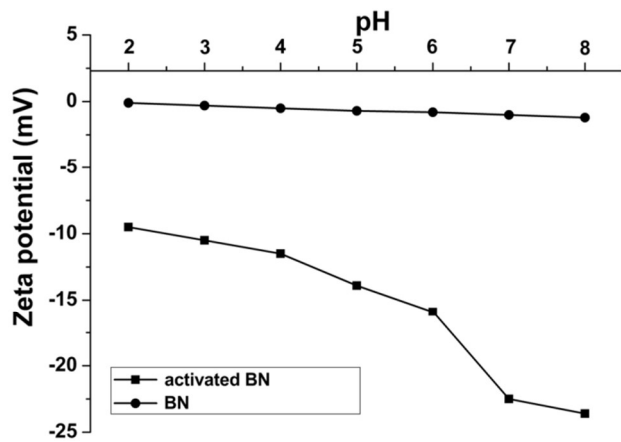
426



427

428 **Figure 3.** Characterization of pore structure of the two adsorbents. a) Nitrogen  
429 adsorption/desorption isotherms, b) the corresponding pore size distributions obtained by  
430 NLDFT method.

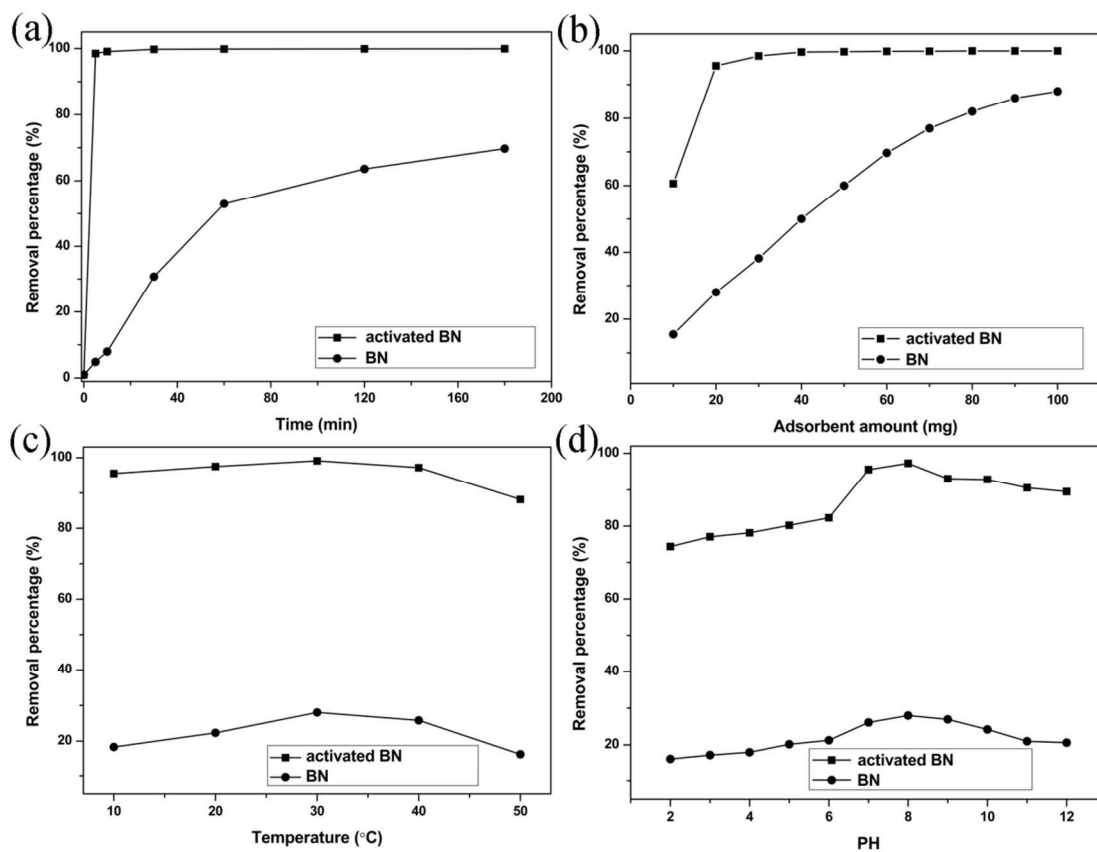
431



432  
433

**Figure 4.** Zeta potential vs. pH values of the activated BN and the BN fibers.

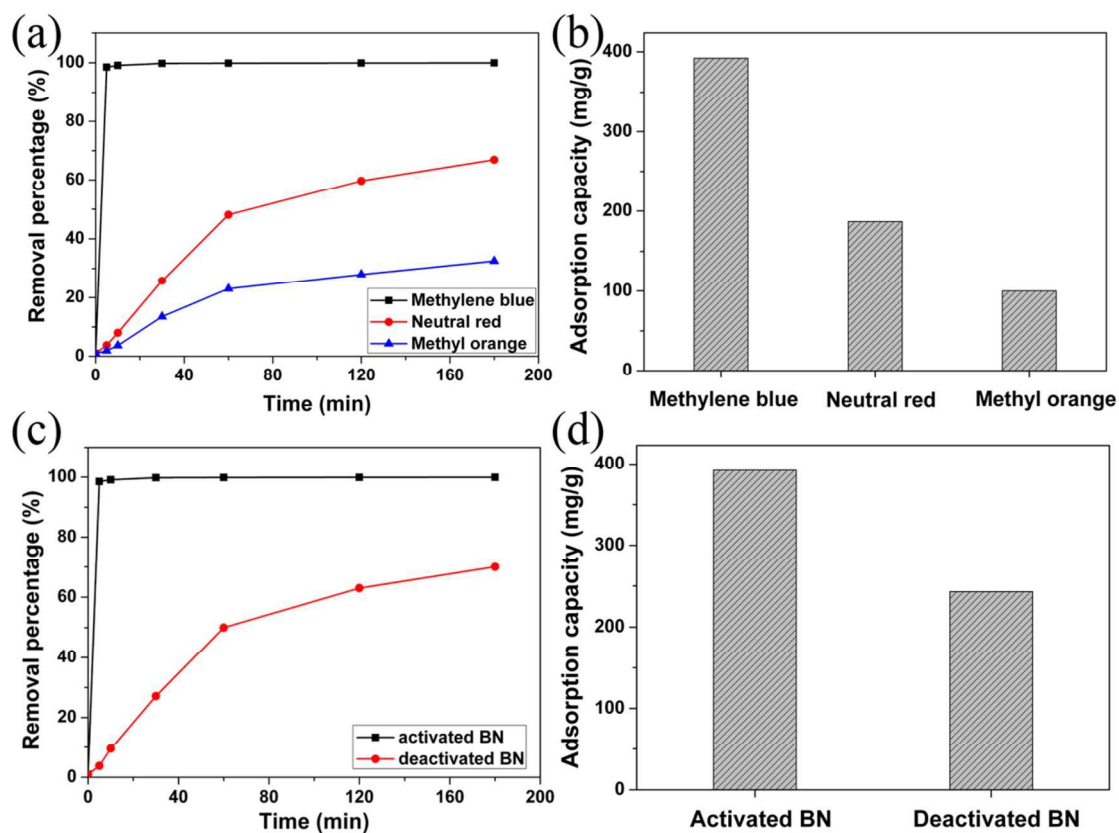
434



435  
436 **Figure 5.** (a) Adsorption rate of MB on the two adsorbents (pH value: 8, adsorbent dosage: 60  
437 mg, adsorption temperature: 30 °C, dye concentration: 25 mg/L). (b) Effect of adsorbent dosage  
438 for adsorption of MB (pH value: 8, contact time: 180 min, adsorption temperature: 30 °C, dye  
439 concentration: 25 mg/L). (c) Effect of temperature for adsorption of MB (pH value: 8, contact  
440 time: 180 min, adsorbent dosage: 20 mg, dye concentration: 25 mg/L). (d) Effect of pH value for  
441 adsorption of MB (Contact time: 180 min, MB concentration: 25 mg/L, temperature: 30 °C,  
442 adsorbent dosage: 20 mg).

443

444



445

446 **Figure 6.** (a) Comparison of adsorption rates of methylene blue, neutral red, and methyl orange

447 on the chemically activated BN (pH value: 8, adsorbent dosage: 60 mg, adsorption temperature:

448 30 °C, dye concentration: 25 mg/L, solution volume: 250 mL), respectively. (b) The

449 corresponding comparison of adsorption capacities for the different styles of dye. (c)

450 Comparison of adsorption rates of methylene blue on the activated BN and deactivated BN,

451 respectively. (d) The corresponding comparison of adsorption capacity.

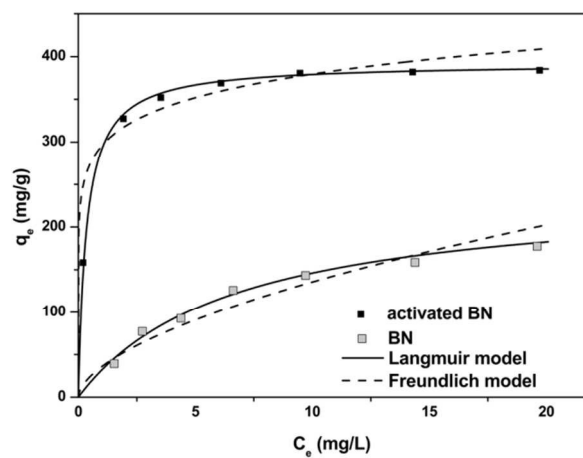
452

453

454

455

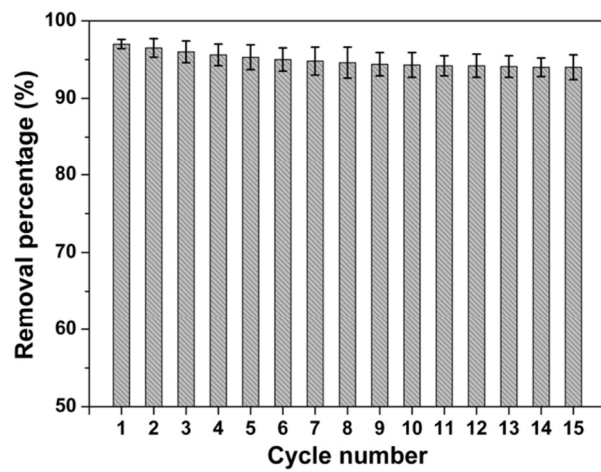
456



457

458 **Figure 7.** Adsorption isotherms of MB on the two adsorbents. Contact time: 180 min, pH: 8,  
459 temperature: 30 °C, dye concentration: 25 mg/L.

460



461

462 **Figure 8.** Reusability of the activated BN regenerated by calcinations.

463

464